Do the Traditional and Modified Latarjet Techniques Produce Equivalent Reconstruction Stability and Strength?

Joshua W. Giles, Gabor Puskas, Mark Welsh, James A. Johnson and George S. Athwal

Am J Sports Med 2012 40: 2801 originally published online September 28, 2012
DOI: 10.1177/0363546512460835

Do the Traditional and Modified Latarjet Techniques Produce Equivalent Reconstruction Stability and Strength?

Joshua W. Giles,* BESc, Gabor Puskas,† MD, Mark Welsh,* BScE,
James A. Johnson,* PhD, and George S. Athwal,*‡ MD, FRCSC
Investigation performed at the Bioengineering Research Laboratory,
Hand and Upper Limb Centre, St Joseph's Health Centre, London, Ontario, Canada

Background: The Latarjet procedure has been described as a reconstructive option for instability associated with substantial glenoid bone defects. A modification, termed the *Congruent-Arc*, is thought to improve glenoid reconstruction through better articular congruency and greater bone reconstitution. The strengths of these techniques, however, have not been reported.

Purpose/Hypothesis: To compare the fixation stability, strength, glenoid vault load transfer, and joint contact between the Classic and Congruent-Arc techniques. The authors hypothesized that the Classic Latarjet would exhibit inferior joint contact characteristics while having greater stability and strength and more normal glenoid vault strain.

Study Design: Controlled laboratory study.

Methods: Sixteen shoulder specimens (8 pairs) were tested by loading the glenohumeral joint with the glenoid intact, following creation of a 25% anterior bone defect, and after random assignment to the Classic or Congruent-Arc Latarjet techniques. Specimens were mounted to a testing apparatus that allowed concentric, centralized loading and loading 30° anterior on the glenoid rim. Cyclic loading (100 cycles at 1 Hz) was applied with a staircase protocol (50, 100, 150, and 200 N). Graft interface displacement and glenoid load transfer, quantified in terms of strain, were recorded during loading. Contact was quantified during 50-N loading using a thin pressure sensor. After cyclic loading, specimens were loaded to failure, defined as 5 mm of graft interface displacement.

Results: The 30° loading $\geq$100 N resulted in significantly greater graft displacement ($P < .004$) in the Congruent-Arc group as compared with the Classic (mean displacement range, 0.9-2.6 vs 0.1-0.5 mm, respectively). Failure testing yielded a significantly ($P = .010$) greater ultimate strength for the Classic (557 N) as compared with the Congruent-Arc (392 N). Load-transfer measurements demonstrated that neither technique's glenoid vault strain values significantly differed from intact ($P \geq .076$). Both techniques resulted in contact areas significantly less than intact ($P < .035$); however, the Congruent-Arc trended toward better contact characteristics ($P = .074$).

Conclusion: The Congruent-Arc results in significantly poorer fixation stability as compared with the Classic technique but did more closely reproduce intact joint contact, which may yield more favorable long-term outcomes.

Clinical Relevance: Care must be taken in balancing the consideration of initial fixation stability and joint contact for the Congruent-Arc and Classic Latarjet, as these factors have opposing implications for each of the 2 reconstructions' outcomes.

Keywords: Latarjet; instability; shoulder; dislocation; Bristow; coracoid

Anterior shoulder instability with associated substantial glenoid bone defects has been found to have high recurrence rates when managed with isolated capsulolabral repair.[3-5,13] This has increased interest, among sports medicine surgeons, in the use of bone block procedures such as the Latarjet coracoid transfer. The technique of the Latarjet coracoid transfer has remained largely unchanged since its initial description in 1954[11]; however, renewed interest in the procedure has led to modifications such as that described by de Beer et al[7] in 2009.

The Latarjet procedure as originally described, termed the *Classic Latarjet*, consists of osteotomizing the coracoid at the elbow formed by its ascending and horizontal pillars, between the coracoclavicular ligaments and the pectoralis minor insertion. The osteotomized coracoid is then transferred to the

‡Address correspondence to George S. Athwal, MD, FRCSC, Bioengineering Research Laboratory, Hand and Upper Limb Centre, St Joseph's Health Centre, 268 Grosvenor Street, London, Ontario, Canada, N6A 4L6 (e-mail: gathwal@uwo.ca).

*Bioengineering Research Laboratory, Hand and Upper Limb Centre, St Joseph's Health Centre, Ontario, Canada.

†Balgrist University Hospital, University of Zurich, Zurich, Switzerland.

One or more of the authors has declared the following potential conflict of interest or source of funding: Fixation screws and guides were donated by Arthrex. As well, indirect funding support was provided by a grant from the Natural Science and Engineering Research Council of Canada.

The American Journal of Sports Medicine, Vol. 40, No. 12
DOI: 10.1177/0363546512460835

anterior glenoid and fixated such that its lateral surface is parallel and flush with the articulation (see Figure 1A). de Beer's modification to this classic technique is termed the *Congruent-Arc Latarjet*. This technique involves rotating the coracoid graft 90° about its longitudinal axis and transferring it such that the inferior surface reconstitutes the glenoid articulation (see Figure 1B). This alteration was originally advocated because of the observation that the inferior curvature of the coracoid would result in improved glenohumeral congruity and thus stability.[7] Armitage et al[1] confirmed this observation through a computed tomography anatomy study that found that the radius of the curvature of the inferior coracoid surface was not statistically different ($P > .05$) from the curvature of the native anterior glenoid rim (13.6 vs 13.8 mm, respectively).

Subsequently, a number of studies have investigated the Congruent-Arc Latarjet's proposed advantages on the basis of joint stability and anatomic match between the glenoid and coracoid. Ghodadra et al[8] compared the Congruent-Arc and Classic Latarjet on the basis of loading mechanics in a cadaveric model and found that the Congruent-Arc provided significantly better results for both contact pressure and area. Additional data from Armitage et al,[1] Hantes et al,[9] and Ljungquist et al[12] demonstrated that the Classic Latarjet can reconstitute 29% to 36% of glenoid width, whereas a Congruent-Arc graft can reconstruct a significantly greater defect, up to 53%. This finding illustrates the Congruent-Arc Latarjet's ability to treat large glenoid defects; however, when this is considered in conjunction with coracoid thickness (8.4-11 mm or ~60% of its width[1,2,12,15]), it becomes apparent that the Congruent-Arc produces a cantilevered geometry and has a smaller contact area with the native glenoid, which may predispose it to graft fixation issues (see Figure 1, C and D).

The purpose of this study, therefore, was to investigate and compare the fixation stability, failure strength, and loading mechanics of a coracoid graft transferred using the Congruent-Arc and Classic Latarjet techniques. It was hypothesized that, because of its geometry, the Congruent-Arc Latarjet would exhibit poorer fixation stability and failure strength with a more abnormal pattern of load transmission to the intact glenoid vault as compared with the Classic technique but would result in improved contact mechanics.

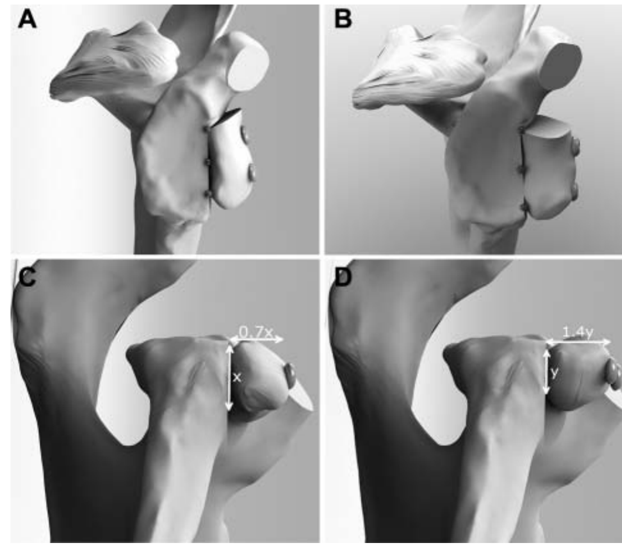

Figure 1. (A) The Classic Latarjet with the transferred coracoid oriented with the lateral surface flush with the glenoid articulation. (B) The Congruent-Arc Latarjet with the transferred coracoid oriented with the inferior curvature flush with the glenoid articulation. Note that both A and B demonstrate the locations of the inferior, middle, and superior digitizations made to monitor graft-glenoid interface displacements. A view from inferior of the Classic Latarjet (C) and Congruent-Arc Latarjet (D), respectively, demonstrating the width-thickness relationships where x and y represent the thickness, or dimension contacting the defect, of the 2 coracoid constructs.

MATERIALS AND METHODS

Specimen Preparation and Apparatus

Sixteen fresh-frozen shoulders composed of 8 left and right pairs (average age, 69 years) were tested in this protocol. All specimens were cleared of osteoarthritis, trauma, or prior surgery via a computed tomography scan. Each humerus was transected 10 cm distal to the humeral head. After thawing for 24 hours, specimens were denuded and disarticulated. Further soft tissues on the scapula and humerus were removed, leaving only the glenoid labrum.

The scapula was trimmed and mounted to a custom pot using dental cement (Dentstone; Heraeus Dental, South Bend, Indiana). Alignment ensured that the glenoid articular surface was level with the base of the pot in the superior-inferior and anterior-posterior directions. In addition, the glenoid articular surface was placed 4.5 cm above the surface of the cement to permit strain gauge instrumentation of the glenoid vault (Figure 2). To accurately and reproducibly align the humerus, vertical and horizontal Kirschner wires were placed in the greater tuberosity while the specimen was articulated in neutral rotation and 30° of glenohumeral abduction. The Kirschner wires were used to guide positioning of the humerus into a custom pot and then removed before testing.

After fixation, the scapula was instrumented with a uniaxial strain gauge (Micro-Measurements; Vishay Precision Group, Raleigh, North Carolina) oriented with its primary axis aligned in the mediolateral direction and located on the anterior glenoid vault (Figure 2). This active strain gauge on the glenoid vault was located directly anterior, in line with the equator of the inferior glenoid circle, and medial to the glenoid rim by 60% of the glenoid width. Sixty percent of glenoid width was chosen as the criterion for medial placement of the gauge to account for variations in specimen size. This gauge was paired with a temperature compensation strain gauge, in a half Wheatstone bridge configuration, mounted in an area free from loading located on the posterior surface of the junction between the spine and acromion. The purpose of the strain gauge was to quantify the changes in load transfer in the plane of loading for the various conditions tested.

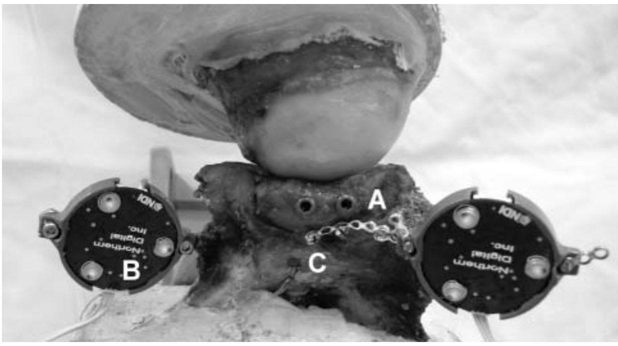

Figure 2. A shoulder specimen mounted to the testing apparatus with complete instrumentation in place. This figure illustrates the orientations in which the scapula and humerus were potted, as well as the position of the specimen during eccentric rim loading. Also note the coracoid graft oriented in A, the Congruent-Arc fashion; B, the 6 degree-of-freedom optical markers tracking the graft and native glenoid after Latarjet reconstruction; and C, the positioning of the anterior glenoid vault strain gauge.

A 6 degree-of-freedom (DOF) optical tracking marker (Optotrak Certus; NDI, Waterloo, Ontario, Canada) was fixed to the intact scapula to provide a reference for displacement readings recorded throughout testing. The marker was placed at the posteroinferior aspect of the glenoid vault, 1 cm medial to the glenoid rim (Figure 2). This location was chosen as it was near enough to the glenoid to eliminate erroneous displacements resulting from flexing of the scapula while being far enough away not to interfere with reconstructions or the testing apparatus.

The scapula and humerus pots were mounted to a material testing apparatus (Instron Materials Testing System, Norwood, Massachusetts). The scapula was attached to a custom positioning apparatus mounted to the system's base while the humerus was fixed to the Instron's primary actuator. The positioning apparatus was capable of adjusting the scapula's superior-inferior and anterior-posterior location as well as the version angle between 0° and 30°. Once both pots were mounted, their alignment was adjusted and the glenohumeral joint was articulated. A constant 5-N load was applied and final adjustments to the scapula's superior-inferior and anterior-posterior location were made until displacement of the Instron actuator reached its maximum, indicating that the humerus was centered in the deepest point of the glenoid.

Testing Protocol

The protocol was designed to assess the fixation stability, failure strength, and load transfer of a coracoid graft using the Congruent-Arc and Classic Latarjet techniques and to compare them with the intact glenoid. Therefore, the conditions tested included the intact glenoid, 25% anterior bony glenoid defect, and the Congruent-Arc or the Classic Latarjet coracoid transfers. An anterior defect comprising 25% of the bony glenoid width was chosen as it represents a common defect that is also of sufficient size to initiate instability as demonstrated by Yamamoto et al.[18]

A repeated-measures study design was used to test each state on each specimen; however, because of the destructive nature of the testing of each Latarjet technique, paired specimens were used. For each specimen pair, the Latarjet technique was randomly selected and balancing was used to ensure each technique was tested equally on each side.

After testing was performed on the intact specimen, the 25% bony glenoid defect was created. This was accomplished by measuring the maximum anteroposterior glenoid width with digital calipers. A line parallel to the superior-inferior axis was marked at a position posterior to the anterior glenoid rim by the equivalent of 25% of its width. The bony defect was then created using a microsagittal saw ensuring that the cut was parallel to the superior-inferior axis as is seen clinically with instability-related glenoid bone loss.[14] Testing was then performed.

The previously selected Latarjet reconstruction technique was performed with the coracoid oriented as described by Latarjet[11] and de Beer et al[7] for the Classic and Congruent-Arc techniques, respectively. Coracoid graft fixation was achieved by decorticating the surface in contact with the anterior glenoid vault and rigidly fixing it using two 3.75-mm cannulated screws (Arthrex, Naples, Florida). Three digitizations were taken along the graft–intact glenoid interface at the most superior, middle, and most inferior points (Figure 1, A and B). Each of these points was recorded with respect to the coracoid marker and the previously described glenoid marker simultaneously, which resulted in 3 pairs of points, located at the graft-glenoid interface, which were initially coincident. Because the 2 markers were rigidly fixed relative to each bone, the 3-dimensional coordinates of the 3 points remained constant throughout testing. However, by tracking the relative motion between the coracoid and glenoid optical markers, it was possible to calculate the distance between the pairs of points, which were initially coincident. This calculated distance was termed *interface displacement* and was calculated continuously throughout testing.

For all test conditions, the joint was configured in neutral internal-external rotation and 30° of glenohumeral abduction. Conditions were tested using 2 cyclic, staircase loading protocols each with a distinct force vector—first with a concentric, centralized load and, second, with an eccentric, glenoid rim load. For the concentric protocol, the load was applied by stabilizing the scapula in 0° of version and maintaining it in the centralized location described above. For the eccentric protocol, the eccentric, glenoid rim load was achieved by anteriorly translating and rotating the humeral head 30° relative to the scapula such that the apex of the head was positioned on the glenoid rim (or reconstructed rim). The concentric and eccentric loading protocols were selected to replicate relevant clinical situations of a humeral head well centralized, as during postoperative sling immobilization, and a humeral head translated anteriorly in a position immediately preceding dislocation, respectively. For the 25% defect state, the second protocol was not performed as no rim existed for load application. In both protocols, a staircase design was used whereby 100 cycles of each load were applied at

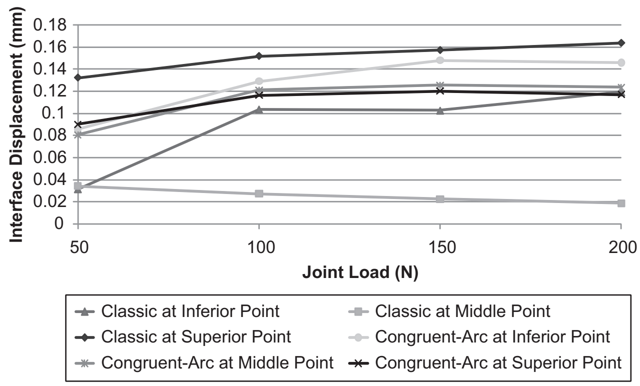

Figure 3. Mean interface displacements, during concentric loading, between the native glenoid and a Classic or Congruent-Arc Latarjet reconstruction. Note that measurements are displayed for inferior, middle, and superior positions. A significant difference was observed between Congruent-Arc and Classic Latarjet at the middle point during 200-N loading. Note that standard deviations are omitted from the figure for clarity and listed below. Standard deviations (in mm) at loads from 50 to 200 N are as follows: superior point, Classic = 0.10-0.19, Congruent-Arc = 0.09-0.13; middle point, Classic = 0.11-0.13, Congruent-Arc = 0.08-0.14; inferior point, Classic = 0.08-0.10, Congruent-Arc = 0.08-0.18.

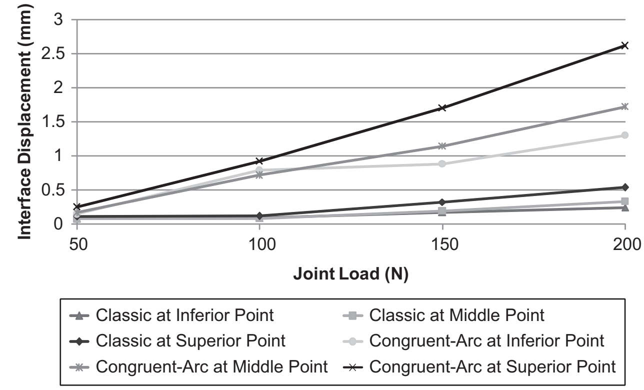

Figure 4. Interface displacements (mean ± 1 standard deviation), during eccentric loading, between the native glenoid and a Classic or Congruent-Arc Latarjet reconstruction. Note that measurements are displayed for inferior, middle, and superior positions. Significant differences were observed between Congruent-Arc and Classic Latarjet at the superior and middle points from 100 N and up ($P \leq .004$ and $P \leq .044$, respectively). Note that standard deviations are omitted from the figure for clarity and listed below. Standard deviations (in mm) at loads from 50 to 200 N are as follows: superior point, Classic = 0.11-0.34, Congruent-Arc = 0.36-1.19; middle point, Classic = 0.11-0.23, Congruent-Arc = 0.24-0.90; inferior point, Classic = 0.12-0.30, Congruent-Arc = 0.32-1.45.

a rate of 1 Hz. The applied load magnitudes were 50, 100, 150, and 200 N.

After 50-N concentric cyclic loading, a contact pressure sensor (Tekscan, Boston, Massachusetts) was placed in the glenohumeral joint and a recording was taken while compressing the joint with a constant 50-N force. This was done to quantify the contact area that existed in each joint condition.

After both protocols were completed, failure strength testing was conducted. This test was performed with the scapula in 0° of version and with the point of load application on the reconstructed rim. Ramp loading to failure at a rate of 0.5 mm/sec was conducted until the coracoid graft reached failure. Failure was predefined as occurring when graft displacement, at its interface with the glenoid, reached 5 mm relative to its initial position.

Outcome Variables and Statistical Analyses

Five outcome variables were assessed. The primary outcome was coracoid graft-to-glenoid interface displacements. This outcome was recorded as the final interface displacement of the graft during the 100th cycle at each loading level and was used to compare the fixation stability of the 2 Latarjet techniques. As this outcome could not be assessed for the intact condition, because the continuous nature of the intact glenoid rim would not yield meaningful displacements, a secondary displacement outcome was used. This outcome was obtained by using the humeral head displacements quantified by displacement of the actuator of the testing machine. This outcome provided data regarding the gross displacement of the intact glenoid/reconstruction at the point of load application and thus allowed comparison between these states as well as between Latarjet techniques. The failure strength outcome was quantified as the load required to displace the graft-glenoid interface by 5 mm from its initial position (as measured by the tracking system).

The glenoid vault strain and Tekscan contact maps were used to assess alterations in joint load-transfer and contact mechanics, respectively. Strain was assessed as the magnitude of strain in the glenoid vault at the 100th cycle for each loading level. To remove noise, a threshold was applied to the Tekscan contact maps, and the area of contact was quantified in mm^2 for each condition.

Statistical analyses for each outcome variable were composed of a series of paired samples *t* tests with significance defined as $P < .05$.

RESULTS

Graft-Glenoid Interface Displacement

During central loading, mean superior, middle, and inferior graft displacements for the Congruent-Arc and Classic techniques were $\leq 0.2 \pm 0.2$ mm and $\leq 0.2 \pm 0.2$ mm, respectively, for all loading levels (Figure 3). The techniques did not differ at any of the 3 measurement points for any load level except the middle point of the Congruent-Arc, which was greater than the Classic at 200 N loading (0.1 ± 0.1 mm; $P = .048$). During eccentric rim loading, interface displacement significantly differed between techniques for loads ≥100 N for the superior ($P \leq .004$) and middle ($P \leq .044$)

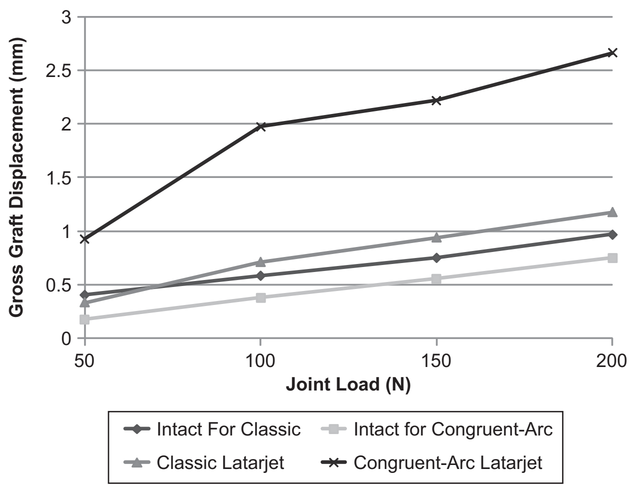

Figure 5. Gross graft displacements (mean ± 1 standard deviation) during eccentric loading. States shown include the Classic and Congruent-Arc Latarjet techniques as well as their respective intact conditions, termed *Intact for Classic* and *Intact for Congruent-Arc*. Note that measurements represent gross graft displacement as measured by the materials testing machine. Significant differences were observed between Congruent-Arc and Intact for Congruent-Arc at 100 N and above ($P \leq .023$). Note that standard deviations are omitted from the figure for clarity and listed below. Standard deviations (in mm) for loads from 50 to 200 N: Intact for Classic = 0.07-0.25; Classic Latarjet = 0.10-0.33; Intact for Congruent-Arc = 0.60-0.71; Congruent-Arc Latarjet = 0.85-1.03.

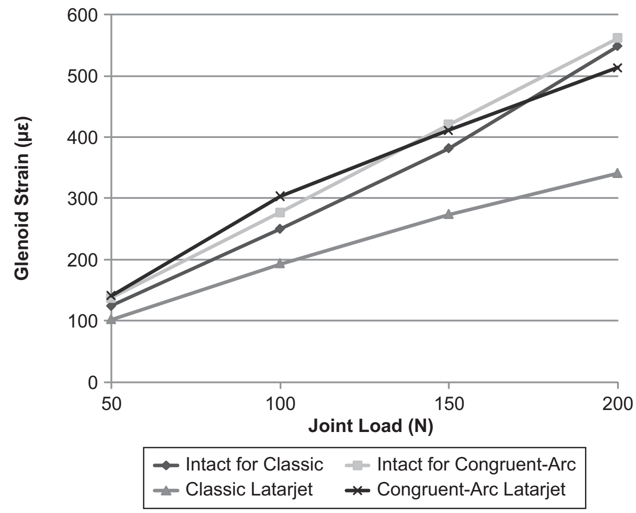

Figure 6. Anterior glenoid vault strain (mean ± 1 standard deviation) during eccentric loading. States shown include the Classic and Congruent-Arc Latarjet techniques as well as their respective intact conditions, termed *Intact for Classic* and *Intact for Congruent-Arc*. Note that standard deviations are omitted from the figure for clarity and listed below. Standard deviations (in microstrain [με]) for loads from 50 to 200 N: Intact for Classic = 5.25×10^{-5} to 16.30×10^{-5}, Classic Latarjet = 9.47×10^{-5} to 28.40×10^{-5}, Intact for Congruent-Arc = 6.69×10^{-5} to 19.60×10^{-5}, Congruent-Arc Latarjet = 9.46×10^{-5} to 33.60×10^{-5}.

measurement points, whereas inferior was different only at 200 N ($P = .049$) (Figure 4). With 0.9 to 2.6 mm of displacement at the superior point and 0.7 to 1.7 mm at the middle point, the Congruent-Arc Latarjet resulted in greater displacements than the Classic technique, whose displacements ranged from 0.1 to 0.5 mm over the same loading range.

Gross Graft Displacement

Overall graft displacement for central loading yielded no significant differences between Latarjet techniques and their intact control condition, with magnitudes ranging from 0.3 to 1.4 mm and the largest difference being 1.1 ± 3.0 mm ($P = .353$). During eccentric loading, graft displacements after the Classic Latarjet did not differ significantly from the intact glenoid rim (≤0.2 mm, $P \geq .064$), whereas the Congruent-Arc technique resulted in significantly greater graft displacement at 100 N (1.6 ± 1.6 mm, $P = .023$), 150 N (1.7 ± 1.2 mm, $P = .005$), and 200 N (1.9 ± 1.4 mm, $P = .005$) (Figure 5).

Graft Failure Strength

Comparison of graft failure strength indicated that the Congruent-Arc Latarjet fails at a significantly lower load than the Classic technique ($P = .010$). The maximum loads for the Congruent-Arc Latarjet and the Classic Latarjet were 392 ± 150 N and 557 ± 135 N, respectively.

Strain and Contact Maps

Strain data indicated that the magnitude of load transferred through the glenoid vault did not significantly differ among Congruent-Arc Latarjet, Classic Latarjet, or intact conditions, for either concentric or eccentric loading at any load level ($P \geq .076$) (Figure 6). The difference in the contact area reestablished by the 2 Latarjet techniques did not significantly differ (59.9 ± 117.3 mm^2; $P = .192$) (Table 1). In addition, both techniques resulted in contact areas significantly less than the intact state (Congruent-Arc, 89.0 ± 96.4 mm^2, $P = .035$; Classic, 153.4 ± 104.4 mm^2, $P = .004$); however, the Congruent-Arc trended toward an increased contact area as compared with the 25% glenoid defect state (61.6 ± 83.1 mm^2, $P = .074$), whereas the Classic Latarjet did not (–30.3 ± 70.2 mm^2, $P = .262$).

DISCUSSION

The Latarjet reconstruction has become a staple in the management of complex anterior shoulder instability following the recognition by Burkhart and De Beer[5] that instability involving a substantial glenoid defect is not amenable to isolated capsulolabral repair. Although the Latarjet, as originally described, has been reported as successful, modifications to the technique have been developed. de Beer et al[7] described the Congruent-Arc modification, which rotates the coracoid graft 90° such that the inferior surface is flush

TABLE 1
Contact Area for the Intact, 25% Anterior Glenoid Bony Defect, and Latarjet Reconstruction Conditions Grouped by Reconstruction Technique[a]

	Condition, Classic Reconstruction Specimens			Condition, Congruent-Arc Reconstruction Specimens		
	Intact	25% Bony Defect	Latarjet	Intact	25% Bony Defect	Latarjet
Mean contact area, mm^2	572.3	449.1	418.9	567.8	417.1	478.8
±1 standard deviation	58.6	76.6	134.6	71.0	136.3	124.2

[a]Significant comparisons were observed between the Classic Latarjet reconstruction and its corresponding intact state (P = .004) as well as the Congruent-Arc Latarjet and its intact condition (P = .035). In addition, the contact area of the Congruent-Arc approached a statistically significant increase as compared with the defect condition (P = .074).

with the glenoid. One direct comparison and several clinical and biomechanical studies have demonstrated the efficacy of both Latarjet techniques.[6,10,16] These investigations, however, have not scrutinized each technique's coracoid graft mechanics, despite geometric differences in the reconstructions that may alter fixation stability, strength, and loading mechanics.

The results of this study found no significant differences in coracoid graft-glenoid interface displacement between techniques during concentric, centralized loading. This lack of effect, despite increasing applied loads, indicates that a flush-mounted graft with a 25% glenoid deficiency likely does not carry a significant portion of joint forces resulting from concentric, centralized loading. Eccentric rim loads, however, cause marked interface displacements, which are significantly greater for the Congruent-Arc technique than the Classic at all load levels above 50 N. These differences average 420% across all locations and load levels, ranging from 90% greater displacement than the Classic at 50 N to 770% at 200 N.

In addition, the Congruent-Arc Latarjet demonstrated significant differences in interface displacement between consecutive loads as low as 50 and 100 N, whereas the Classic technique did not permit significant increases until the 100- to 150-N interval. This indicates that not only does the Congruent-Arc technique allow greater graft displacement but also that these increases are significant at lower loads. Moreover, analysis of the superior, middle, and inferior measurement point data revealed that both Latarjet techniques induce a superior graft tilt, which increases with load. This tilting in the graft presents as progressively greater displacements from inferior to superior. This tilt, however, is far more pronounced with the Congruent-Arc reconstruction. This effect is likely due to the shape of the glenoid articulation, which, when loaded, causes greater forces to be experienced centrally. This causes greater load transmission to the superior aspect of the graft, which is located more centrally at approximately the equator of the glenoid.

No significant differences were observed in terms of gross graft displacement during concentric, centralized loading. Eccentric loading, which was intended to model a position just preceding dislocation, resulted in marked increases in displacement beyond the intact level with the Congruent-Arc technique. These findings of increased displacement with the Congruent-Arc technique are similar to the results from the glenoid-graft interface assessment. By comparing the graft-glenoid interface displacements to the gross graft displacements for the Congruent-Arc Latarjet, it is evident that the mode of displacement is directed medially, with minimal anterior tilting or anteversion. This indicates that the geometry and point of load application (Figure 1B) of the Congruent-Arc reconstruction produces increased loads and accompanying displacements but does not suffer from a noticeable graft rotation.

The final measure of fixation stability, the failure load, demonstrated that the Congruent-Arc technique was significantly weaker (30% weaker) than the Classic technique. In fact, the Congruent-Arc technique was unable to support a load equivalent to 1 body weight, which is commonly experienced in the shoulder.[17] The cause of this disparity in failure strength can be directly linked to the comparative geometry of the 2 Latarjet constructs. The most important factor is the shape of the coracoid—specifically, the coracoid's width and thickness, as it is rectangular in cross section, with its width always being greater than its thickness.[1] This consistent width-thickness relationship, therefore, causes the Congruent-Arc orientation to produce a reconstructed "rim" that is much further from the native glenoid than with the Classic Latarjet, thus resulting in greater loads at the interface. In addition, in assessing the relative coracoid graft thicknesses, it was observed that the Congruent-Arc graft-defect interface is much thinner than the Classic, thus resulting in less of a base to support the increased loads caused by the graft's width. These 2 factors together cause a cantilever (or diving board) effect, which significantly reduces the Congruent-Arc Latarjet's strength. With the results of the 3 stability-related outcomes for both Latarjet techniques in mind, it is clear that concentric, centralized glenohumeral loading represents a critical factor in shielding the Latarjet from excessive load postoperatively and promoting successful healing and bony union.

Glenoid vault strain after the Latarjet reconstructions never differed from the intact state; however, although the Congruent-Arc produced values nearly identical to intact state during eccentric loading, the Classic technique resulted in noticeably less strain than the intact state. We speculate that these results are due to the graft orientation, which could result in a complex strain distribution within the glenoid vault. This differs from intact, where continuous bone at the glenoid rim and vault would transmit strain directly medial through the location of measurement. Thus, in comparing the 2 techniques, it is believed that the construct geometry reduces the strain as seen for the Classic Latarjet but remains close to the intact value in the case of the Congruent-Arc, which produces greater interface loading.

Analysis of the contact area demonstrated that the Latarjet techniques did not differ in the amount of contact reestablished and that neither was able to fully restore the intact contact area. In fact, the Classic Latarjet was found to decrease contact area compared with the 25% defect condition. This counterintuitive finding can be explained by the incongruity of the Classic Latarjet with the native glenoid, which causes the initial contact of the humeral head to be with the stiff cortical bone of the coracoid graft over a smaller area. This contact with the incongruous graft resulted in a characteristic pressure concentration between the graft and humeral articular cartilage. Also, our findings for the Congruent-Arc Latarjet differ from those of Ghodadra et al,[8] who found that this coracoid orientation was indeed able to fully restore intact contact. Despite this disagreement, the Congruent-Arc Latarjet may be considered a better option for restoring contact as, unlike the Classic technique, it did approach a significant increase as compared with the 25% glenoid defect. This improved joint contact represents an important factor in support of using the Congruent-Arc Latarjet as it may decrease the adverse effects of abnormal joint stresses in the long term.

Some limitations can be associated with this in vitro biomechanical investigation. The greatest limitation of this study was related to the study design itself, which used paired specimens instead of fully repeated measures because of the destructive nature of testing each reconstruction. Related to this, only 1 combination of abduction and rotation was tested to ensure acquisition of a complete data set; however, testing of multiple configurations may have provided a more complete description of the 2 constructs' properties. Another limitation was the inability to characterize the complete strain field in the glenoid vault, which would have allowed a more detailed comparison of load transfer. Also, the results of this study represent time zero and thus cannot be extrapolated to determine final clinical results. Finally, this study examined only the bony contributions to Latarjet strength; the effects of the soft tissues (labrum and capsule) were not studied.

CONCLUSION

This study compared the effects of the Classic and Congruent-Arc Latarjet reconstructions on coracoid graft loading mechanics, fixation stability, and failure strength. The data indicate that the Congruent-Arc Latarjet results in significantly greater graft displacements and lower clinical failure load as compared with the Classic Latarjet, which may have implications on the risk of graft failure. However, the Congruent-Arc Latarjet produces more favorable joint contact mechanics when compared with the Classic Latarjet, and this must also be a strong consideration when evaluating the use of either reconstructive option. Finally, the small displacements observed during concentric glenohumeral loading emphasize the importance of maintaining a centralized humeral head position postoperatively to promote Latarjet healing and bony union.

REFERENCES

1. Armitage MS, Elkinson I, Giles JW, Athwal GS. An anatomic, computed tomographic assessment of the coracoid process with special reference to the Congruent-Arc Latarjet procedure. *Arthroscopy*. 2011;27(11):1485-1489.
2. Bhatia DN, de Beer JF, du Toit DF. Coracoid process anatomy: implications in radiographic imaging and surgery. *Clin Anat*. 2007;20(7):774-784.
3. Boileau P, Villalba M, Héry JY, Balg F, Ahrens P, Neyton L. Risk factors for recurrence of shoulder instability after arthroscopic Bankart repair. *J Bone Joint Surg Am*. 2006;88(8):1755-1763.
4. Boone JL, Arciero RA. Management of failed instability surgery: how to get it right the next time. *Orthop Clin North Am*. 2010;41(3):367-379.
5. Burkhart SS, De Beer JF. Traumatic glenohumeral bone defects and their relationship to failure of arthroscopic Bankart repairs: significance of the inverted-pear glenoid and the humeral engaging Hill-Sachs lesion. *Arthroscopy*. 2000;16(7):677-694.
6. Burkhart SS, De Beer JF, Barth JR, Cresswell T, Roberts C, Richards DP. Results of modified Latarjet reconstruction in patients with anteroinferior instability and significant bone loss. *Arthroscopy*. 2007;23(10):1033-1041.
7. de Beer J, Burkhart SS, Roberts CP, Van Rooyen K, Cresswell T, du Toit D. The Congruent-Arc Latarjet. *Tech Shoulder Elbow Surg*. 2009;10(2):62-67.
8. Ghodadra N, Gupta A, Romeo AA, et al. Normalization of glenohumeral articular contact pressures after Latarjet or iliac crest bone-grafting. *J Bone Joint Surg Am*. 2010;92(6):1478-1489.
9. Hantes ME, Venouziou A, Bargiotas KA, Metafratzi Z, Karantanas A, Malizos KN. Repair of an anteroinferior glenoid defect by the Latarjet procedure: quantitative assessment of the repair by computed tomography. *Arthroscopy*. 2010;26(8):1021-1026.
10. Hovelius L, Sandstrom B, Sundgren K, Saebo M. One hundred eighteen Bristow-Latarjet repairs for recurrent anterior dislocation of the shoulder prospectively followed for fifteen years: study I—clinical results. *J Shoulder Elbow Surg*. 2004;13(5):509-516.
11. Latarjet M. Treatment of recurrent dislocation of the shoulder. *Lyon Chir*. 1954;49(8):994-997.
12. Ljungquist KL, Butler RB, Griesser MJ, Bishop JY. Prediction of coracoid thickness using a glenoid width-based model: implications for bone reconstruction procedures in chronic anterior shoulder instability. *J Shoulder Elbow Surg*. 2012;21(6):815-821.
13. Provencher MT, Ghodadra N, Romeo AA. Arthroscopic management of anterior instability: pearls, pitfalls, and lessons learned. *Orthop Clin North Am*. 2010;41(3):325-337.
14. Saito H, Itoi E, Sugaya H, Minagawa H, Yamamoto N, Tuoheti Y. Location of the glenoid defect in shoulders with recurrent anterior dislocation. *Am J Sports Med*. 2005;33(6):889-893.
15. von Schroeder HP, Kuiper SD, Botte MJ. Osseous anatomy of the scapula. *Clin Orthop Relat Res*. 2001;383:131-139.
16. Wellmann M, Petersen W, Zantop T, et al. Open shoulder repair of osseous glenoid defects: biomechanical effectiveness of the Latarjet procedure versus a contoured structural bone graft. *Am J Sports Med*. 2009;37(1):87-94.
17. Westerhoff P, Graichen F, Bender A, et al. In vivo measurement of shoulder joint loads during activities of daily living. *J Biomech*. 2009;42(12):1840-1849.
18. Yamamoto N, Muraki T, Sperling JW, et al. Stabilizing mechanism in bone-grafting of a large glenoid defect. *J Bone Joint Surg Am*. 2010;92(11):2059-2066.